

# We are IntechOpen, the world's leading publisher of Open Access books Built by scientists, for scientists

5,500

Open access books available

134,000

International authors and editors

165M

Downloads

Our authors are among the

154

Countries delivered to

TOP 1%

most cited scientists

12.2%

Contributors from top 500 universities



WEB OF SCIENCE™

Selection of our books indexed in the Book Citation Index  
in Web of Science™ Core Collection (BKCI)

Interested in publishing with us?  
Contact [book.department@intechopen.com](mailto:book.department@intechopen.com)

Numbers displayed above are based on latest data collected.  
For more information visit [www.intechopen.com](http://www.intechopen.com)



# The Quantification of Crystalline Phases in Materials: Applications of Rietveld Method

Cláudia T. Kniess<sup>1,2</sup>, João Cardoso de Lima<sup>2</sup> and Patrícia B. Prates<sup>2</sup>

<sup>1</sup>*Nove de Julho University – UNINOVE – São Paulo – SP*

<sup>2</sup>*Federal University of Santa Catarina – UFSC – Florianópolis – SC  
Brazil*

## 1. Introduction

The materials have their properties defined by the chemical composition and the microstructure presented on them. The quantification of crystalline phases is a key step in determining the structure, properties and applications of a given material. Therefore, the study of the amount of crystalline phases present in a material represents an important parameter to control the microstructure and the correlation of the properties associated with the developed stage in the process. The distribution of phases or microstructure depends on the manufacturing techniques, sintering process, raw materials used, equilibrium reactions, kinetics and phase changes. The characterization of crystalline microstructure, regarding the density, atomic distribution and unit cell dimensions, contributes to the control of the manufacturing process. It is also the basis for phase identification, structure, porosity and evaluating the performance of materials. Within this context, the book's chapter entitled "Quantification of Crystalline Phases in Materials: Applications of the Rietveld Method" aims to present and discuss some topics related to methods for quantification of crystalline phases in materials using the technique of X-ray diffraction, especially in the case of ceramic materials. It will examine various methods of quantification of crystalline phases described in the literature, but the focus will be applications of the Rietveld Method.

## 2. Materials and microstructure

The modern construction techniques, the growing competitiveness in international markets and the technological renewal, demand products that meet the basic requirements of high quality and low cost. The knowledge of raw materials and the effect on the processing and properties stages of the final product are necessary to achieve these requirements (KNISS, 2005).

The materials have their properties defined by the chemical composition and the microstructure they exhibit. These characteristics are influenced by the selection of raw materials and the manufacturing process, mainly the sintering process. The research advances in materials engineering aspects seek to correlate microstructural features, including crystalline and amorphous phases, porosity, etc., with properties of interest, like

mechanical strength, coefficient of thermal expansion, density, among others. For most materials, the identification and quantification of amorphous and crystalline phases is crucial in determining the structure, properties, and applications of a material.

Solid materials can be classified according to the regularity by which their atoms or ions are arranged in relation to each other (PADILHA, 1997). The structure of solid material is a result of the nature of their chemical bonds, which defines the spatial distribution of atoms, ions or molecules. Solid materials can be crystalline or amorphous. The concept of crystal structure is related to organization of atoms geometry. The vast majority of materials, commonly used in engineering, particularly metals, shows a well defined geometric arrangement of their atoms, forming a crystalline structure.

A crystalline material is the one in which the atoms are located in a repeated arrangement or that is periodically over long atomic distances; that is, there is long-range order, so, when the solidification occurs the atoms will place themselves in a three dimensional repetitive pattern, in which each atom is connected to its nearest neighbor atoms. All metals, many ceramic materials and certain polymers were crystalline structures under normal solidification conditions (CALLISTER, 2002).

From the concept of crystal structure, where it is possible to describe a set of repetitive atomic, ionic or molecular positions, arises the concept of unit cell. A unit cell is defined as the smallest portion of the crystal that still retains its original properties. Through the adoption of specific values associated with the units of measure on the axes of references, defined as network parameters, and the angles between these axes, it can be obtained unit cells of various kinds.

The atomic structures of materials can not be regularly arranged as in crystalline networks. Such structures are called amorphous or vitreous (NAVARRO, 1991). This type of structure, however, is not completely disordered. It is formed by constitutive blocks arranged in a disorderly way. But the structure of these blocks is regular. Thus, it can be said that the glassy structures have long-range disorder and short-range order.

The ceramics and glasses are distinguished from other materials – metals and polymers – essentially by the type of chemical bonds that each one has. (KINGERY *et al.*, 1976). Regardless of the final products, the ceramic process begins with the selection of mineral or synthetic raw materials. We can classify the ceramic materials in two large groups: the traditional ceramics, using mostly natural raw materials, with a predominance of clays nature, and advanced ceramics, in which raw materials are essentially synthetic (FONSECA, 2000).

The amount of crystalline phases present in a ceramic material is an important parameter to control the microstructure and the properties correlation associated to the phase developed in the process (BORBA, 2000). Another focus of the quantitative analysis of phases is the measure of crystallinity, in other words, the fraction of crystalline phases present in the sample. In the case of ceramic materials, where the thermal process generates different amounts of crystalline phases, the content of residual amorphous phase is an important parameter, not only as physical characterization of the product, but to correlate it with the mechanical properties and kinetic studies of crystallization.

### 3. Application of X-ray diffraction techniques to quantification of phases in materials

There are many techniques for characterization of polycrystalline materials (X-ray diffraction, differential thermal analysis, thermogravimetric analysis, infrared spectroscopy, scanning electron microscopy, transmission electron microscopy, nuclear magnetic resonance spectroscopy, ultraviolet spectroscopy, etc), each of which is most suitable for a particular purpose and the others can be used to supplement the findings obtained by other technique. The characterization methods that make use of X-ray or neutron diffraction are particularly interesting for: (i) index of crystalline phases, (ii) refinements of unit cell, (iii) determination of crystallite size and network micro-deformations, (iv) quantitative analysis of phases, (v) determination of crystal structures, (vi) refinement of crystal structures, (vii) determination of preferred orientation (texture), etc. (PAIVA-SANTOS, 1990).

The technique of X-ray diffraction is still considered the most suitable for quantitative analysis of phases. However, the percentage of phases present in the material (amorphous and crystalline), quantification of the glassy phase, depends on the manufacturing techniques, sintering process, raw materials used, equilibrium reactions, kinetics and phase changes. The characterization of crystalline microstructure, with respect to the density, atomic distribution and dimensions of the unit cell, contributes to the control of the manufacturing process.

#### 3.1 X-ray diffraction principles

The X-ray diffraction (XRD) represents the phenomenon of interactions between the incident X-ray beam and the electrons of the atoms of a material component, related to the coherent scattering.

The technique consists in the incidence of radiation on a sample and in the detection of the diffracted photons, which constitute the diffracted beam.

The scattering and the resulting X-ray diffraction is a process that can be analyzed at different levels. In the most basic of them, there is the X-ray scattering by an electron. This scattering can be coherent or incoherent. In coherent scattering, the scattered wave has a definite direction, the same phase and energy in relation to the incident wave. It is an elastic collision. In incoherent scattering, the scattered wave has no definite direction (CULLITY, 1978). It does not keep the phase or energy (this is called Compton Effect). The collision is inelastic, and the energy for the difference between the incident wave and the wave scattered translates into temperature gain (vibration of the atom).

When an X-ray beam, with a certain frequency, focuses on an atom, it behaves as a scattering center, and vibrates at the same frequency as the incident beam, spreading in all directions. When the atoms are arranged in a lattice, this incident beam will undergo a constructive interference in certain directions, and destructive in others. The constructive interference of scattered radiation occurs when the path difference of successive planes scattered beam is equal to an integer number of wavelength (KLUG & ALEXANDER, 1954).

Bragg's law is a geometric interpretation of the diffraction phenomenon of atoms arranged in a lattice. In a material where the atoms are arranged periodically in space, characteristic of

crystalline structures, the phenomenon of X-ray diffraction occurs in the scattering directions that satisfy Bragg's Law, Equation (3.1). This Law is a consequence of the periodicity of the network and is not associated with each particular atom, or different atomic numbers (CULLITY, 1978).

Assuming that a monochromatic beam of a certain wavelength ( $\lambda$ ) incident on a crystal at an angle  $\theta$ , we have (KLUG & ALEXANDER, 1954):

$$n \lambda = 2 d \sin \theta \quad (3.1)$$

Where:  $n$  = integer number of wavelength,  $d$  = interplanar distance of the successive crystal planes;  $\theta$  = angle measured between the incident beam and determined crystal planes.

Traditional instruments of measurement are the diffractometer and chambers of single crystals, application of the latter is now restricted to specific situations to determine the crystallographic parameters. In the study of polycrystalline materials in powder form, the radiation is monochromatic and the angle of incidence  $\theta$  is variable. In traditional diffractometer, the diffracted uptake shaft is through a detector, according to a geometrical arrangement known as the Bragg-Brentano geometry (CULLITY, 1978). The X-ray beam falling on the sample, positioned at  $\theta$  is diffracted at the periodicity of the network, and the signal is collected in a detector positioned at  $2\theta$ .

The diffracted beam is usually expressed through peaks that stand out from the background (or baseline), recorded in a spectrum of intensity per second (c.p.s.) versus the angle  $2\theta$  (or  $d$ ), constituting the diffraction pattern of diffractogram.

The intensities obtained at  $2\theta$  angles, represented by the XRD patterns, correspond to the diffraction of the incident beam for a given set of crystal planes, which have the same interplanar distance, each one with Müller hkl indices (hkl reflections). The relative intensity of the peaks is related to the type of atom in the lattice and its occupation number of the atom in the unit cell.

The scattering caused by the electrons in the unit cell results in a complex interference function. The total amplitude of the scattered beam is the sum of the contributions of all electrons, in other words, is proportional to  $Z$  (atomic number). These scattering values are the normalized amplitude of electrons number involved in the angle  $\theta = 0$  and are the atomic scattering factors. In the case of beams scattered in the direction of incidence,  $\theta = 0$ , the rays are in phase and amplitude is added. However, when the angle  $\theta$  is different from zero, the trajectories of the scattered rays are different and the phase difference results in interference. The measure of this phase difference is contained in an exponential factor that defines the change in amplitude as a function of atoms positions. (WILES *et al.*, 1981). The combination of this phase factor and the atomic scattering factor results in the factor of structure (WARREN, 1959) represented by Equation (3.2):

$$F_{hkl} = \sum_{n=1} f_n \exp[2\pi i(hx_n + ky_n + lz_n)] \quad (3.2)$$

where:

$f_n$  = scattering factor for atom  $n$ ;

$x_n, y_n, z_n$  = position coordinates of the  $n$ th atom;

$h, k, l$  = Müller indice;

$f_n = f_0 \exp(-B \sin^2 \theta / \lambda)$ , where  $f_0$  is the scattering of the temperature absolute zero and  $B$  is the medium amplitude of normal vibration to the direction of diffraction.

The position of the peaks is related to the interplanar distances of the phase, i.e., with unit cell parameters. As X-rays penetrate only in the atom electrosphere, the oxidation state of the atom influences the intensity of the diffracted beam. Among the factors that affect the intensity, the main ones are: polarization, temperature, atomic scattering, structure and mass attenuation. (KLUG & ALEXANDER, 1954).

The elevation of the background in the range of  $2\theta$  of 20 and 50° on the amorphous phase, which can be called a "halo" is not constant over the entire angular range, but prevalent in certain areas. The chemical characteristics of the amorphous phase and its form of development, even at short range, determine the shape of "halo". The analysis of the area, shape and position of the "halo" provides information about the degree of ordering of the amorphous phase, being more open as more desorganized phase is (FLEURENCE, 1968).

According to Borba (2000), through the detailed study of the shape and position of the peak, one can get some information about the crystalline phases, related to the structure, crystallite size, heterogeneity and micro-deformations. The width of the diffraction peak is related to the crystallite size and/or existing micro-deformations in the crystal lattice. The peak broadening of one phase of XRD is the indicative of a small crystallite size. This extension can be perceived in a different way in different reflections, indicating that the crystallites grew preferentially in one direction. The asymmetry at large angles may be an indicative of the presence of residual tension, and this tension can vary with crystallographic orientation. The displacement of the positions of the peaks can be associated with macrodeformation for defects and for changes of network parameters produced by disagreements and segregations of atoms dissolved.

Each crystalline compound has a characteristic diffraction pattern, allowing their identification through the angular positions and relative intensities of the diffracted peaks. The identification of crystalline phases is obtained by comparing the XRD with the diffraction patterns of individual phases provided by the ICDD (*International Center for Diffraction Data*), the former JCPDS (*Joint Committee of Powder Diffraction Standards*). It is also possible to calculate the unit cell parameters, assess the degree of crystallinity, and quantify present phases. The quantification of phases from the X-ray diffraction can be related to the intensities of the peaks of XRD pattern. It also represents the characteristics of the crystalline phases existing in the material, characterizing the ratio of these phases.

### 3.1.1 Factors that cause changes in the diffraction pattern

Information on the structure of a material can be obtained through the analysis of some features in the diffraction pattern, which can be summarized in:

- a. the angular position of diffraction lines, which depends on the geometry of the crystal lattice, indicating the size and shape of the unit cell;
- b. intensity of the diffraction lines, which depends on the type of atoms, its arrangement on the crystal lattice and the crystallographic orientation;

- c. shape of the diffraction lines, dependent on the instrumental broadening, particle size, and deformation.

Some factors, instrumental or feature from the samples can influence the diffraction pattern of a sample. According to Klug and Alexander (1954), the instrumental factors for a typical X-ray diffractometer, which influence the profile of the diffraction peaks are:

- a. geometry of the X-ray source;
- b. displacement of the sample;
- c. divergence of the axial X-ray beam;
- d. transparency of the sample;
- e. the purpose of receiving slot;
- f. misalignment of the diffractometer.

The most important non-structural factors that affect the widths, shapes and positions in the peaks of diffraction in the geometries of Bragg-Brentano are (KLUG & ALEXANDER, 1974):

- a. alignment and collimation of the beam, influencing the width and symmetry;
- b. curvature of the diffraction cone, leading to asymmetry of the peaks at high and low angles;
- c. flat shape of the sample surface, producing the peak asymmetry at low angles;
- d. absorption/transparency of the sample, causing displacement of the diffraction peaks;
- e. particle size in the sample and micro-deformations, causing variation in the width and shape of the peaks;
- f. intensity of the incident beam (width and shape of the peaks).

#### 4. Quantitative analysis of crystalline phases

Most of the authors refer to the method of Klug and Alexander (1954) as a predecessor of quantitative analysis, since several other methods have been developed based on it. According to Klug and Alexander, the general equation of quantitative analysis is:

$$I_A = \frac{K_A x_A}{\rho_A (x_A (\mu_A - \mu_M) + \mu_M)} \quad (4.1)$$

where:

$I_A$  = intensity of line  $i$  of unknown phase  $A$ ;

$K_A$  = constant depending on the nature of phase  $A$  and the geometry of the equipment;

$\rho_A$  = density of phase  $A$ ;

$x_A$  = weight fraction of phase  $A$ ;

$\mu_M$  = mass attenuation coefficient of the matrix;

$\mu_A$  = mass attenuation coefficient of phase  $A$ .

There are also known methods of standard addition and external standards, with overlapping peaks (KLUG & ALEXANDER, 1974). With the advancement of computer technology, the method of Rietveld (RIETVELD, 1967, 1969), which is based on the simulation of the diffraction profile from the structures of the phase components in a sample, allowed more information to be extracted from the XRD patterns. Analysing the entire diffraction pattern and using the intensities of each individual angular step, the

method enabled the refinement of complex crystal structures, and therefore it was applied to the provision of quantitative data accurately recognized.

#### 4.1 Rational analysis

The mineralogical composition is defined by the type and quantity of minerals that constitute the material studied. According to the concept of rational mineralogical analysis, described in Coelho (2002), through a combination of quantitative chemical composition (for example, by X-ray fluorescence) and from the determination of qualitative mineralogical analysis (obtained by XRD), we obtain enough theoretic information to solve the problem of quantitative deduction of mineralogical phase, after the relationship with the chemical composition of the phase. There are two widespread procedures for carrying out the calculations needed to solve the problem: the conventional procedure (HALD, 1952) and the procedure using the method IRTEC (FABBRI *et al.*, 1989). The latter method has possible sources of error such as simplifying the theoretical formula of complex phases and errors due to the presence of two or more phases with the same theoretical formula, besides a wide dispersion (standard deviation) in the solutions obtained when the number of phases is less than the number of oxides.

#### 4.2 Internal standard method

The internal standard method is most suitable to be used in case of a large number of samples, where a component must be determined and the composition of the samples varies widely. The advantage of this method is that any crystalline phase can be analyzed without considering all stages, and it was not necessary to consider the amorphous phase (CULLITY 1978). The intensities of characteristic peaks of the phases of the sample components are related to the internal standard peaks, being generalized in a system of linear equations that allow to use overlapping peaks and links to the proportions of the phases. The analysis is performed by adding a P internal standard to the mixture to be analyzed in known amounts, requiring the presence of one or more individual peaks without overlapping with other peaks, being common the use of crystallized material in the cubic system by presenting simple structure and few diffracted peaks (BRINDLEY & BROWN, 1980).

In the analysis of a component of a system where the overlapping lines doesn't occur, and, considering the mass attenuation coefficients of the standard ( $\mu_p$ ) and matrix ( $\mu_M$ ) are different ( $\mu_p \neq \mu_M$ ) (general cases), the intensities of line i of component A and the line K of pattern P follow the Equations (4.2) and (4.3) (CULLITY, 1978):

$$I_{iA} = \left( \frac{K_1 c_A}{\mu_M} \right) \quad (4.2)$$

$$I_{kP} = \left( \frac{K_2 c_P}{\mu_P} \right) \quad (4.3)$$

where:

$c_A$  e  $c_P$  = volume fraction of phase A in the mixture and the standard P;



$K_1, K_2, K_3 = \text{constants.}$

The ratio of two intensities  $I_{iA}/I_{kP}$  leads to the calibration of  $I_{iA}/I_{kP}$  versus  $x_A$ , where  $x_A$  is the fraction of the component to be analyzed according to Equation (4.4):

$$\frac{I_{iA}}{I_{kP}} = K_3 X_A \quad (4.4)$$

### 4.3 Matrix flushing method by chung

Doneda (2000) in his work, refers to the quantitative method developed by CHUNG (1974), from Klug and Alexander equations (1954), called *matrix flushing*, in which a mixture is prepared in a 1:1 ratio of phase to be measured and the corundum standard phase. Chung (1974) elected the corundum as a standard (flushing agent); however, it is also possible to use any other phase not present in the sample. The concentration of a  $x_A$  phase is obtained from the equation:

$$x_A = \left( \frac{x_C}{k_C} \right) \left( \frac{I_A}{I_C} \right) \quad (4.5)$$

where:  $x_C$  is the mass fraction of corundum in the sample;  $I_A$  e  $I_C$  are the intensities of the hkl plane of the A phase and the corundum respectively and  $k_C$  is the constant obtained from the JCPDS.

Equation (4.5) shows that the relations are independent of matrix effects, therefore, to draw a graph  $I_A/I_C$  by  $x_A$ , the slope of the line would be  $x_C/k_C$ . The amorphous phase is determined by the difference between the crystalline phases quantified and total phases in the sample.

### 4.4 External standard method

The external standard method is to prepare a series of mixtures containing the phase to be measured at an increasing rate. The values of intensity of a peak characteristic of various mixtures allow determining the concentration of the phase to be measured (FLEURENCE, 1968).

A condition for the use of this method is the choice of a standard substance P, which has the same characteristic of pure or mixed diffraction.  $I_{p0}$  and  $I_p$  are the intensities of P pure or in the mixture, respectively, measured under the same conditions,  $\mu_p$  and  $\mu_M$  are the mass attenuation coefficients of the pure substance P and the mass attenuation coefficient of the matrix where P is inserted, respectively. The Equation (4.6) relates the intensities of the peaks with the amount of P:

$$\frac{I_p}{I_{p0}} = x_p \frac{\mu_p}{\mu_M} \text{ or } \frac{I_p}{I_{p0}} = \alpha \cdot x_p \quad (4.6)$$

where:  $x_p$  is the proportion of P in the mixture e  $\alpha = \mu_p/\mu_M$  (literature).

#### 4.5 Addition method

The addition method developed by Bragg and Copeland and applied by Fleurence (1968) and Alegre (1965), consists of adding known amounts of a pure phase A to the mixture. This phase A, to be measured, belongs to the system. The methodology consists in measuring the intensities of the peaks of the phases A and B, where B is another phase of the system that will serve as reference for the different samples with increasing amounts of A. The curve  $I_A/I_B$  in the function of  $\alpha$  is generated from the Equation (4.7):

$$\frac{I_A}{I_B} = \left( \frac{\kappa_A \rho_B}{\kappa_B \rho_A x_B} \right) \alpha + \left( \frac{\kappa_A \rho_B x_A}{\kappa_B \rho_A x_B} \right) \quad (4.7)$$

where:  $I_A$  = peak intensity of phase A to be measured;  $I_B$  = amount of peak of phase B; belonging to the sample and acting as a reference;  $\alpha$  = added amount of phase A;  $\rho_A$  e  $\rho_B$  = density of A and B, respectively; and  $x_A$  and  $x_B$  = concentrations, in weight, of A and B, respectively.

According to Borba (2000), as the quantity  $\alpha$  increases, the ratio  $I_A/I_B$  varies linearly, with  $k$ ,  $\rho$  e  $x$  constants. The graph obtained by the ratio  $I_A/I_B$  for  $\alpha$  can be represented by a straight line with coefficient proportional to  $x_A$ . This line intercepts the x-axis at a distant point of origin, so that, when extended,  $x_A$ , ie, the concentration is obtained by graphical extrapolation. This method is similar to the internal standard method, but the added A phase is one of phases of the mixture.

### 5. Quantification of crystalline phases in materials by Rietveld method

Unlike other methods based on the integration of the intensity of characteristic peaks of phases, the method developed by Hugo Rietveld (RIETVELD, 1967, 1969), is applied to the total angular range of the diffraction pattern, increasing the accuracy of the obtained data. The problem of overlapping peaks is minimized, allowing maximum extraction of information from the diffraction pattern.

The Rietveld method involves a refinement of crystal structures, using data from X-ray and neutron diffraction by powder. The term refinement in the Rietveld Method refers to the process of adjusting the model of parameters used in the calculation of a diffraction pattern, to the closest observed. The observed XRD pattern should be obtained in a scanning process step by step with constant growth of  $\Delta 2\theta$  (PAIVA-SANTOS, 2001). The differences between the two diffraction patterns are calculated by the method of least squares, and this minimized the difference as the theoretical model approximates the characteristics of the structure (YOUNG, 1995).

To use the method, you must know the structure of the phases in the mixture with a good degree of approximation and have information such as: type of crystal structure, atomic coordinates, occupation number, oxidation state of atoms, symmetry points, values of factors of isotropic and anisotropic temperature. The basic requirements for the Rietveld refinement are: accurate measurements of intensities given at intervals of  $2\theta$ , an initial model close to the actual structure of the crystal and a model that describes the shape, width and systematic errors in the positions of the Bragg peaks (PAIVA-SANTOS, 1990).

The calculated standard, to fit the observed pattern, provides data on the structural parameters of the material, as well as the parameters of the diffraction profile. The parameters specific to each phase, which vary during the refinement are (YOUNG, 1995):

- a. structural: atomic positions, unit cell parameters, occupancy factors, scale factor, thermal vibration parameters (isotropic and anisotropic) and isotropic thermal parameter general;
- b. non-structural: parameters of the half width (U, V, W), asymmetry,  $2\theta$  zero, preferred orientation and coefficients of the background radiation.

The Rietveld method allows, simultaneously, perform unit cell refinement, refinement of crystal structure, microstructure analysis, quantitative analysis of phases and determination of preferred orientation (RIELLO *et al.*, 1995).

With the advancement of computer technology, the Rietveld method has allowed more information to be extracted from XRD patterns. From the analysis of all the diffraction pattern and using the individual intensities of each angular step, the method enabled the refinement of complex crystal structures, and therefore can be applied to the provision of quantitative data accurately recognized (KNISS *et al.*, 2007).

Over the past three decades, the version of the computer program originally developed by RIETVELD (1967, 1969) has been extensively modified. The program DBWS (WILES & YOUNG, 1981) was probably the most widely used until 1995. In the version DBWS 9411 (YOUNG *et al.*, 1998), the entry data of theoretical model can be given through various crystallographic databases, such as: *Inorganic Crystal Structure Database (ICSD)*, *Power Diffraction File (PDF) - International Centre for Diffraction Data (ICDD)*, *Structure Reports, Cambridge Structure Data Base (CSD)* e *Metals Crystallographic Data File (CRYSTMET)*.

The GSAS program (General Structure Analysis System), developed by Larson and Von Dreele (1998) at Los Alamos National Laboratory, has great flexibility for single crystal data, powder diffraction, neutron diffraction. It is widespread in the scientific community and constant updated.

The commercial programs available usually refer to the X-Ray diffraction equipment suppliers. The best known are the High Score Plus (Panalytical) and the Topas (Bruker AXS GmbH - Germany). The Siroquant is from CSIRO, Research Centre in Brisbane (Australia).

Young (1995) lists the most commonly used programs available at universities for the refinement of crystal structures by the Rietveld method, as shown in Table 5.1.

Computer Program	Reference
Rietveld	Rietveld (1969)
Rietveld	Hewat (1973)
PFLS	Toraya e Marumo (1980)
DBW	Wiles e Young (1981)
X-ray Rietveld System	Baerlocher (1952)
LHPM1	Hill e Howard (1986)
GSAS	Larson e Von Dreele (1988)
FullProf	Rodrigues-Carvajal (1990)

Table 5.1. Most widely used programs in universities to the refinement of crystal structures.

### 5.1 Refinement methodology

Obtaining data suitable for the Rietveld refinement requires attention to the choice of material, which must have small particle size and a minimum of preferred orientation. The sample should be prepared so that the surface is smooth and homogeneous, to avoid the effect of surface roughness.

In order to obtain optimal results, the conditions of data collection should be determined prior to the refining. The main factors to determine are the wavelength, the collimation of the beam, the angular range and angular distance between the steps and counting time. The choice of appropriate values for the count time  $T$  (which defines the intensity and for angular interval of step (which in a given interval determines the number of steps  $N$ ) depends on the experimental conditions and characteristics of the studied material.

With the choice of a theoretical model of the structure through a database, and subsequent entry of the theoretical data in the program, followed by the step of refining the experimental parameters. The variables contain in the input the data necessary for the construction of the calculated diffraction pattern, ie, data on the crystal structure of the material. The main data are:  $2\theta$  limits, wavelengths of radiation used, specification of the background radiation, the space group symbol, symbol and valence of each atom (used for entering tables scattering factors) and number of phases.

The main parameters that can be adjusted simultaneously in the refinement are (CARVALHO, 1996):

- a. scale factor: is the correction of proportionality between the calculated and observed diffraction patterns. The refinement of the scale factor is directly related to the amount of phase;
- b. baseline (background): is corrected from data collected in the same XRD pattern and interpolation between these points. It is important to understand the behavior of the baseline, since this provides information about the presence of amorphous phases in the sample and can be included in a routine of quantification of involved phases. The fit of the background equation uses a polynomial up to fifth grade and instrumental aberrations can be considered during the refinement;
- c. peak profile: set of analytical functions that are modeled effects related to the profile. Some analytical equations are proposed to correct these effects, such as the Gaussian and the Lorentzian equation and the equation that corrects the asymmetry. The width and position of the peaks are related to the characteristics of crystallite size and cell, respectively;
- d. cell parameters: the cell parameters can be fitted by Bragg's Law, where the interplanar distance of successive planes of the crystal ( $d$ ) is related to the Miller indices and therefore the parameters of cell ( $a, b, c, \alpha, \beta, \gamma$ ). The indexing of the peaks is made taking into account the parameters of the cell and the intensity calculated, which shows a certain advantage over conventional techniques, for all the parameters that influence the discrepancy in the values of " $d$ ", are handled jointly with the intensities;
- e. factor of structure: the variable parameters of this factor are the atomic positions, the isotropic or anisotropic temperature factors and the occupation number;
- f. offset: parameters for correction of displacements due to leakage of the focal point of the optical diffractometer;

- g. factors of temperature: can absorb deficiencies in the model for the background radiation, absorption and surface roughness, and show discrepancies with the values determined by single crystal diffraction experiments. Therefore, the factors of temperature can be set to values obtained from the literature and an overall temperature factor refined;
- h. preferential orientation: correlation of problems generated in the sample preparation.

In the study by Post and Bish (1989), the authors suggest the refining steps for any crystalline sample. If the analyzed sample has several crystalline phases, models of atomic structures should be entered for each phase. The study shows that the first few cycles of least squares should be performed with the coefficients of the baseline and the scale factor set, and then several cycles with the inclusion of other parameters should be performed. During the refinement, it is essential to observe the differences between the spectra of the calculated and observed patterns, so that problems can be detected, like background settings and peak of the profile irregularities. The spectral differences are also important for the verification phase that may not have been included in the refinement. Post and Bish (1989) and Young (1995) consider the control chart refinement important for checking the quality of refinement.

## 5.2 Output file and refinement evaluation

Through the Equation (5.1) one can calculate the  $x_B$  concentration of a given B phase, after the refinement of all  $i$  phases.

$$x_B = \frac{F_B(ZMV)_B}{\sum_i [S_i(ZMV)_i]} \quad (5.1)$$

where: F is the scale factor refined by the program; Z is the number of formula units per unit of unit cell, M is the mass of the formula unit, V is the volume of the unit cell.

The refinement can be assessed by verification of the structural parameters and profile obtained, the comparison of results with those obtained for single crystals and the observation of plot of calculated and observed patterns, as well as the residuals obtained.

The quality of refinement is verified by numerical statistical indicators that are used during the iterative process (calculations) and after its termination, in order to check whether the refinement proceeds satisfactorily. Table 5.2 presents the metrics most commonly used in the refinements using the Rietveld method (POST E BISH, 1989; YOUNG, 1995; GOBBO, 2003).

Equation	Indicator
$R_F = \sum   (I_K ("OBS"))^{1/2} - (I_K (CALC))^{1/2}   / \sum (I_K ("OBS"))^{1/2}$	R - Structure Factor
$R_B = \sum   I_K ("OBS") - I_K (CALC)   / \sum (I_K ("OBS"))$	R - Bragg
$R_P = \sum   y_i (OBS) - y_i (CALC)   / \sum y_i (OBS)$	R Profile
$R_{WP} = \{ \sum w_i (y_i (OBS) - y_i (CALC))^2 / \sum w_i (y_i (OBS))^2 \}^{1/2}$	R - Profile Adjust
$S = [S_y / (N-P)]^{1/2} = R_{WP} / R_{EXP}$	Goodness of Fit = GOF = S
$R_{EXP} = [(N-P) / \sum W_i y_{i0}^2]^{1/2}$	R - Expected

Table 5.2. Statistical indicators most frequently used in the refinements based on the Rietveld method.

1.  $I_K$  is the intensity of Bragg K reflection at the end of each cycle of refinement. In the expressions for  $R_F$  and  $R_B$ , the "obs", an observed, is placed between quotation marks because the  $I_K$  is computed as Rietveld (1969);
2.  $N$  = number of parameters being refined;  $P$  = number of observations  
Source: GOBBO, (2003).

The quality of refinement is verified by two numerical statistical indicators  $R_P$  and  $R_{WP}$ , comparative parameters between theoretical and experimental XRD patterns, which can be used to monitor the convergence of the model.  $R_P$  and  $R_{WP}$  should reach a value of  $R_{EXP}$  to consider the model acceptable. The residue  $R_{WP}$  considers the error associated with each intensity value by the number of counts, using the weighting factor  $w(2\theta)$ . The value of  $R_{WP}$  for good results is 2-10%, while the typical values obtained range from 10-20%. To evaluate the goodness of fit, we compare the final values of  $R_{WP}$  with the expected value of the error ( $R_{EXP}$ ). The expected error is derived from the statistical error associated with the measured intensities.  $R_{EXP}$  is related to the quality of the experimental diffractogram, this value being smaller is better (BORBA, 2000). In practice, differences of up to 20% between  $R_{EXP}$  and  $R_P$  are acceptable.  $R_{WP}$  is a statistical indicator that represents the best approach, since the numerator is the residual minimized in the least squares procedure. The factors that modify the  $R_{WP}$  are differences in the peaks (as the width) and the background radiation.

From the mathematical point of view,  $R_{wp}$  is one of the indices that best reflect the progress of refinement, because the numerator has the residue that is minimized.  $R_{wp}$  is the index that should be analyzed to see if the refinement is converging. If  $R_{wp}$  is decreasing, then the refinement is successful. At the end of the refinement it should not be more varied, meaning that the minimum has been reached. If  $R_{wp}$  is increasing, then some parameter (s) is (are) diverging from the actual value and refinement should be discontinued for a more detailed analysis of the parameters being refined.

$S$  is called the "goodness-of-fit (GOF)" (Equation 5.2) and should be close to 1,0 at the end of refinement, meaning that nothing else can be improved because the  $R_{wp}$  has reached the limit that can be expected to those measured diffraction data. The *goodness-of-fit* should be equivalent to 1,0 in a perfect refinement. In practice less than five figures reflect an optimized refinement.

$$S = R_{WP}/R_{EXP} \quad (5.2)$$

where:  $R_{EXP}$  is the value statistically expected to  $R_{WP}$ .

All these indices provide subsidies to the user to judge the quality of refinement. However, none of them is related to the crystal structure but only to the profile of the XRD pattern. To assess the quality of the refined structural model, one should calculate the  $R_{BRAGG}$ , which is described as a function of the integrated intensities of the peaks (PAIVA-SANTOS, 2005).

$$R_{BRAGG} = 100[(\sum |I_o - I_c|)/(\sum I_o)] \quad (5.3)$$

where:  $I_o$  is the intensity observed in the angular position;  $I_c$  is the intensity calculated in the angular position.

As the integrated intensity is related to the crystal structure (types of atoms, atomic positions and displacement), this index is to be considered when evaluating the quality of the refined model of the crystal structure.

## 6. Applications of Rietveld method: Case study

Several studies in the literature addressing the application of the Rietveld method in the quantification of crystalline phases of materials, such as: Borba (2000); Paiva-Santos (2001); Gobbo (2003); Kniess, *et al.* (2009a); Kniess, *et al.* (2010).

In this part of the chapter, we will discuss two case studies in which the Rietveld method was used in the refinement and quantification of crystalline phases of materials.

The first case described in the work of Kniess, *et al.* (2007), refers to the refinement and quantification of crystalline phases of mineral coal bottom ash, residue resulting from combustion of coal in thermoelectric plants to produce electricity.

The second case described in Kniess, *et al.* (2009b), deals with the study of the structural refinement and quantification of crystalline phases of ceramic bodies materials.

### 6.1 CASE 1 – By-product mineral coal bottom ash

#### 6.1.1 Characterization of the problem

The Jorge Lacerda thermoelectric plant, located at Santa Catarina State, Brazil, uses mineral coal, extracted from the Criciúma region (Santa Catarina State). The burning of coal mineral results in two types of residues: fly and bottom ashes. The first residue has been used as by-products in the cement industries while the second one, which represents almost 50% of the total residues generated by the thermoelectric plants, up to now has no industrial applications causing a serious problem for the environment.

The physical, chemical and mineralogical properties of coal ash are compatible with various raw materials used in ceramic industries coating, which indicates a possibility of partial or full utilisation for this residue. The mineral coal ash has the market value of at least four times smaller than many commercial minerals commonly used as raw materials. The production cost can be reduced both in terms of raw material is a residue of low cost, but also in its physical presentation, whereas the particle size distribution of the residual range of about 5-200 $\mu\text{m}$ .

The mineral coal bottom ash is composed mainly of  $\text{SiO}_2$  and  $\text{Al}_2\text{O}_3$  (about 80% by weight). The measured X-ray diffraction (XRD) pattern for coal bottom ash has shown that it is composed majority by low quartz ( $\text{SiO}_2$ ) and mullite ( $3\text{Al}_2\text{O}_3 \cdot 2\text{SiO}_2$ ).

#### 6.1.2 Mineralogical and chemical characterization of mineral coal bottom ash

The mineral coal bottom ash used in the study was submitted to drying in an oven as 110° C during 24 hours. The percentage of moisture in this particular batch was 20%. Removing the fraction with detectable levels of carbonaceous material macroscopically, because the presence of carbon generates gases that can remain attached, making the sample homogeneity.

Chemical analysis of industrial by-product was carried out in a XRF spectrometer Philips PW 1400 with Rh tube. To obtain the sample, glass was prepared by using a mixture of lithium tetraborate and lithium metaborate as a flux. Chemical analysis of coal bottom ash is presented in Table 6.1. Some trace elements such as Ba, Pb, Cu, Cr and Ni were determined by atomic absorption spectrometry, Table 6.2.

Constituents	Coal Bottom Ash (%)
SiO <sub>2</sub>	54,04
Al <sub>2</sub> O <sub>3</sub>	25,19
Fe <sub>2</sub> O <sub>3</sub>	4,61
CaO	2,26
MnO	0,03
MgO	1,41
TiO <sub>2</sub>	0,91
Na <sub>2</sub> O	0,86
K <sub>2</sub> O	0,95
P <sub>2</sub> O <sub>5</sub>	0,22
Losses in fire	8,52

Table 6.1. Chemical analysis in oxides, of the mineral coal bottom ash.

Constituent	Coal Bottom Ash (ppm)
Ba	299
Nb	27
Zr	286
Sr	168
Rb	71
Pb	27
Zn	32
Cu	34
Ni	48
Cr	224

Table 6.2. Chemical analysis of mineral coal bottom ash. (trace elements).

The mineralogical analysis of coal ash was performed on its powder using the X-ray diffractometric method. The equipment used was a Philips diffractometer, model X'Pert, Copper K<sub>α</sub> radiation ( $\lambda = 1,54056 \text{ \AA}$ ), power of 40 kV e 30 mA, nickel filter in the secondary optic. The byproduct was crushed in a mortar, sieved and separated fractions with particle size less than 45  $\mu\text{m}$ . The analysis conditions were: 0,02° for the step, step time 2s and measuring range in 2 $\theta$ , of 10 to 90°.

The figure 6.1 shows the X-ray diffractogram of bottom coal ash. The presented crystalline phases were identified using the JCPDS (1981) and ICSD (1995) database. The analysis of the XRD pattern shows that the bottom ash is formed by the crystalline phases quartz (SiO<sub>2</sub> - JCPDS 5-490), mullite (Al<sub>2</sub>Si<sub>6</sub>O<sub>13</sub> - JCPDS 15-776), magnetite (Fe<sub>3</sub>O<sub>4</sub> - JCPDS 19-629) and hematite (Fe<sub>2</sub>O<sub>3</sub> - JCPDS 13-534).



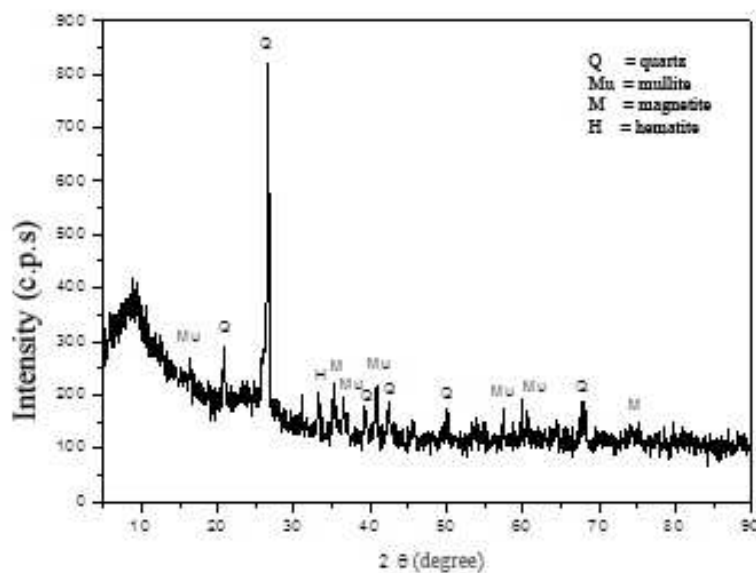


Fig. 6.1. X-ray diffractogram of mineral coal bottom ash.

### 6.1.3 Structural refinement and quantification of crystalline phases by the Rietveld method

The crystalline phases identified from mineral coal bottom ash were quantified using the Rietveld Method (RIETVELD, 1965, 1965). The software used was DB8K98. The graphic display of the plots of the XRD patterns (simulated and experimental) was obtained through the program DMPLLOT.

In order to estimate the relative amount of each crystalline phase, the XRD experimental spectrum was simulated using the Rietveld method for structure refinement. Crystallographic data (atomic coordinates, space group, cell parameters and temperature factor) used were those available in the archives ICSD numbers 174, 23726, 20596 e 15840 for all phases identified, presented in Table 6.3. These are the input information for the refinement, which consists in comparing the structure of theoretical models and the observed spectrum.

Table 6.4 present the refined crystallographic data for the crystalline phases present in mineral coal bottom ash. It is observed that the values of network parameters were refined and the atomic positions and isotropic temperature factors of atoms remained constant after the refinement.

The intense background in the diffractogram of coal bottom ash (Figure 6.1), which was set in the simulation proces, was not regarded as an amorphous phase, since it is difficult to measure it separately. The curves of experimental and simulated pattern (Figure 6.2) showed a good agreement, resulting in the following percentages of relative phases: quartz (34,94%), mullite (64,22%), magnetite (0,38%) and hematite (0,46%).

Phase	Space Group	Lattice Parameters (Å)	Temperature Factor ( $B_o$ )	Atomic Positions
Quartz (SiO <sub>2</sub> ) ICSD # 174 PDF # 05-490	P 32 2 1 S (No. 154)	a = 4.913 b = a c = 5.405	$B_o = 0$ $B_o = 0$	Si (3a), x = 0.4698, y = 0.0, z = 0.0 O (6c), x = 0.4141, y = 0.2681, z = 0.1188
Mullite (Al <sub>2.35</sub> O <sub>4.82</sub> Si <sub>0.64</sub> ) ICSD # 23726 PDF # 15-776	P B A M (No. 55)	a = 7.566 b = 7.682 c = 2.884	$B_o = 0.43$ $B_o = 0.51$ $B_o = 0.49$ $B_o = 0.49$ $B_o = 0.97$ $B_o = 0.92$ $B_o = 1.40$ $B_o = 0.84$	Al (2a), x = y = z = 0.0 Al (4h), x = 0.2380, y = 0.2945, z = 1/2 Al (4h), x = 0.3512, y = 0.1590, z = 1/2 Si (4h), x = 0.3512, y = 0.1590, z = 1/2 O (4g), x = 0.3929, y = 0.2808, z = 0.0 O (4h), x = 0.1420, y = 0.0777, z = 1/2 O (2d), x = 0.0, y = 1/2, z = 1/2 O (4h), x = 0.0509, y = 0.4482, z = 1/2
Magnetite (Fe <sub>3</sub> O <sub>4</sub> ) ICSD #20596 PDF No. 19-629	F D 3 M (No. 227)	a=b=c=8.400	$B_o = 0$ $B_o = 0$ $B_o = 0$	Fe (8a), x = y = z = 1/8 Fe (16d), x = y = z = 1/2 O (32e), x = y = z = 0.258
Hematite (Fe <sub>2</sub> O <sub>3</sub> ) ICSD # 15840 PDF No. 13-534	R -3 C H (No. 167)	a = 5.038 b = a c = 13.772	$B_o = 0$ $B_o = 0$	Fe (12c), x = y = 0.0, z = 0.3553 O (18e), x = 0.3059, y = 0.0, z = 1/4

Table 6.3. Theoretical crystallographic data for the crystalline phases present in mineral coal bottom ash.

Phase	Space Group	Lattice Parameters (Å)	Temperature Factor ( $B_o$ )	Atomic Position
Quartz (SiO <sub>2</sub> )	P 32 2 1 S (No. 154)	a = 4.919 b = a c = 5.414	$B_o = 0$ $B_o = 0$	Si (3a), x = 0.4698; y = 0.0, z = 0.0 O (6c), x = 0.4141; y = 0.2681, z = 0.1188
Mullite (Al <sub>2.35</sub> O <sub>4.82</sub> Si <sub>0.64</sub> )	P B A M (No. 55)	a = 7.563 b = 7.706 c = 2.890	$B_o = 0.43$ $B_o = 0.51$ $B_o = 0.49$ $B_o = 0.49$ $B_o = 0.97$ $B_o = 0.92$ $B_o = 1.40$ $B_o = 0.84$	Al (2a), x = y = z = 0.0 Al (4h), x = 0.2380; y = 0.2945, z = 1/2 Al (4h), x = 0.35120, y = 0.1590, z = 1/2 Si (4h), x = 0.35120, y = 0.1590, z = 1/2 O (4g), x = 0.3929, y = 0.2808, z = 0.0 O (4h), x = 0.1420, y = 0.0777, z = 1/2 O (2d), x = 0.0, y = 1/2, z = 1/2 O (4h), x = 0.0509, y = 0.4482, z = 1/2
Magnetite (Fe <sub>3</sub> O <sub>4</sub> )	F D 3 M (No. 227)	a = 8.401 b = a c = a	$B_o = 0$ $B_o = 0$ $B_o = 0$	Fe (8a), x = y = z = 1/8 Fe (16d), x = y = z = 1/2 O (32e), x = y = z = 0.258
Hematite (Fe <sub>2</sub> O <sub>3</sub> )	R -3 C H (No. 167)	a = 5.048 b = a c = 13.793	$B_o = 0$ $B_o = 0$	Fe (12c), x = y = 0.0 z = 0.3553 O (18e), x = 0.3059, y = 0.0, z = 1/4

Table 6.4. Refined crystallographic data for the crystalline phases present in mineral coal bottom ash.

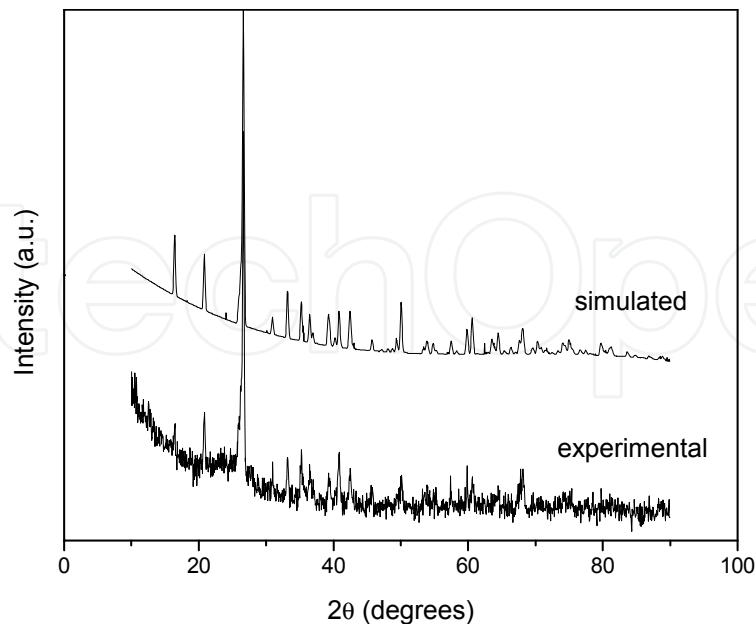


Fig. 6.2. XRD patterns of mineral coal bottom ash: experimental and simulated by the Rietveld Method.

An estimate of the crystallinity of the bottom ash can be performed from the analysis of the integrated intensity areas contained in the diffraction pattern. Subtracting the value of “amorphous area” of the value of “total area” is possible to estimate the value of “crystalline area”. According to this methodology, the bottom ash under study has a crystallinity of 43,10%, or 58,90% of amorphous phase. These results are consistent with results found in the literature (KNISS, 2005).

## 6.2 Case 2 – Ceramic materials

### 6.2.1 Obtaining and characterization of materials

The materials characterized in this study are ceramics materials for covering with addition of clay raw materials (argilominerals) and mineral coal bottom ash, sinterized at 1150° C to 2 hours.

X Ray diffraction analysis of the developed material were obtained with a Philips X'Pert equipment, ( $\lambda = 1,54 \text{ \AA}$ ) through the powder method. Analyses were done with 0,02°/ 2s and  $2\theta$  from 10 to 90°.

Crystalline phases were identified based on JCPDS database.

In order to obtain the crystallographic data, necessary to the structural refinement through the Rietveld Method, the ICSD was used. Input data to the refinement by the Rietveld Method are presented in Table 6.5

The used refinement program was the DBWS 98. DMPLOT program made possible the comparison between the theoretical spectrum and the refined one.

### 6.2.2 Characterization of ceramic materials - Crystalline phases identification

The Figure 6.3 presents the X ray patterns of ceramic material studied: MA, MB, MC, MD. These materials were obtained in the paper described by Kniess *et al.* (2006). Identified crystalline phases (in ceramic materials) are also presented in Figure 6.3.

The Table 6.5 shows theoretical crystallographic data of crystalline phase present in sinterized ceramic materials.

Phase	Lattice parameters (Å)	Atomic Position	Occupation Number	Thermal Isotropic Factors (B <sub>0</sub> )
Quartz ( $\alpha$ -SiO <sub>2</sub> ) ICSD 29210 PDF 05-490 P 32 2 1 S (154)	a = b = 4,913 c = 5,405 $\alpha = \beta = 90$ $\gamma = 120$	Si (3a), x = 0,469, y = 0,0, z = 0,0 O (6c), x = 0,403, y = 0,253, z = 0,122	Si = 1,0 O = 1,0	B <sub>0</sub> (Si) = 0 B <sub>0</sub> (O) = 0
SiO <sub>2</sub> ICSD 34889 PDF 76-0912 P 43 21 2 (96)	a = b = 7,456 c = 8,604 $\alpha = \beta = 90$ $\gamma = 90$	Si (8b), x = 0,326, y = 0,120, z = 0,248 Si (4a), x = 0,410, y = 0,410, z = 0,0 O (8b), x = 0,445, y = 0,132, z = 0,400 O (8b), x = 0,117, y = 0,123, z = 0,296 O (8b), x = 0,334, y = 0,297, z = 0,143	Si (8b) = 1,0 Si (4a) = 1,0 O (8b) = 1,0 O (8b) = 1,0 O (8b) = 1,0	Si (8b) = 2,39 Si (4a) = 2,39 O (8b) = 2,39 O (8b) = 2,39 O (8b) = 2,39
Tridimite (SiO <sub>2</sub> ) ICSD 29343 PDF 75-0638 P 63 2 2 (182)	a = b = 5,01 c = 8,18 $\alpha = \beta = 90$ $\gamma = 120$	Si (4f), x = 0,333, y = 0,667, z = 0,47 O (2c), x = 0,333, y = 0,667, z = 0,25 O (6g), x = 0,425, y = 0,0, z = 0,0	Si (4f) = 1,0 O (2c) = 1,0 O (6g) = 1,0	B <sub>0</sub> (Si) = 0 B <sub>0</sub> (O) = 0
Mullite (Al <sub>2,35</sub> Si <sub>0,64</sub> O <sub>4,82</sub> ) ICSD 23726 PDF 15-776 P B A M (55)	a = 7,566 b = 7,682 c = 2,884 $\alpha = \beta = 90$ $\gamma = 90$	Al (2a), x = y = z = 0,0 Al (4h), x = 0,2380, y = 0,2945, z = 1/2 Al (4h), x = 0,3512, y = 0,1590, z = 1/2 Si (4h), x = 0,3512, y = 0,1590, z = 1/2 O (4g), x = 0,3729, y = 0,2808, z = 0,0 O (4h), x = 0,1420, y = 0,0777, z = 1/2 O (2d), x = 0,0, y = 1/2, z = 1/2 O (4h), x = 0,0509, y = 0,4482, z = 1/2	Al (2a) = 1,0 Al (4h) = 0,34 Al (4h) = 0,34 Si (4h) = 0,33 O (4g) = 1,0 O (4h) = 1,0 O (2d) = 0,41 O (4h) = 0,21	Al (2a) = 0,43 Al (4h) = 0,51 Al (4h) = 0,49 Si (4h) = 0,49 O (4g) = 0,97 O (4h) = 0,92 O (2d) = 1,4 O (4h) = 0,84
Hematite (Fe <sub>2</sub> O <sub>3</sub> ) ICSD 15840 PDF 13-0534 R -3 C H (167)	a = b = 5,038 c = 13,772 $\alpha = \beta = 90$ $\gamma = 120$	Fe (12c), x = 0,0, y = 0,0, z = 0,3553 O (18e), x = 0,3059, y = 0,0, z = 0,25	Fe = 1,0 O = 1,0	B <sub>0</sub> (Fe) = 0 B <sub>0</sub> (O) = 0

Table 6.5. Crystallographic theoretical data of crystalline phase present in sinterized ceramic materials.

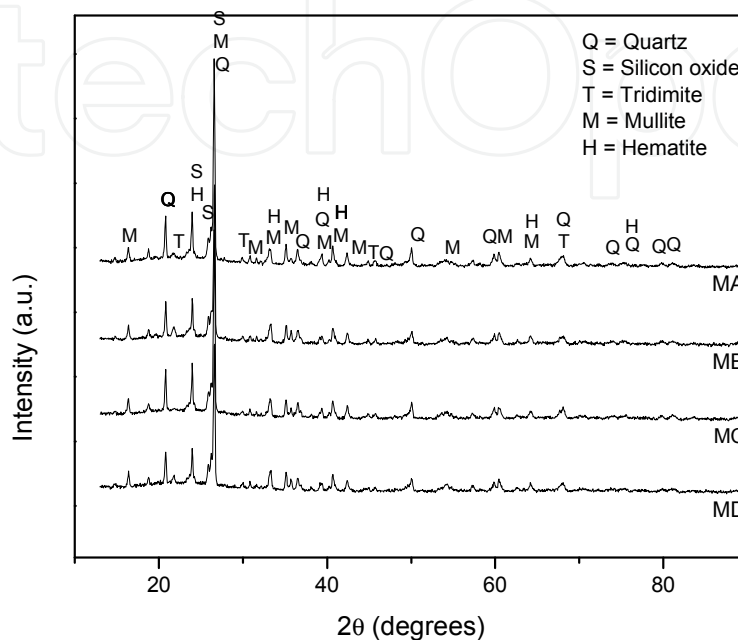


Fig. 6.3. X Ray patterns of ceramic materials, sinterized under the temperature of 1150°C.

### 6.2.3 Crystalline phase quantification by Rietveld method

The Figure 6.4 presents the comparison between the experimental pattern and MA, MB, MC and MD samples simulation, through the Rietveld Method. Materials MA, MB, MC and MD spectrum plotting presented a good approach to the diffraction pattern simulated and the observed one, with a good definition to intensities and peak positions.

Percentage related to crystalline phases, obtained through the Rietveld Method, is presented in Table 6.6, which also presents statistical numeric indicators  $R_p$ ,  $R_{WP}$  e  $R_{EXP}$ .

Crystalline and amorphous phases' characteristics are considered very important factors, which influence mechanical properties of ceramic materials (KNIESS, *et al* 2006). Quartz and mullite were identified as major crystalline components in all four samples. It is possible to observe that the MA material presented the highest percentage of residual quartz after sintering (54,89%). MC material presents the highest percentage of tridymites phase in comparison with the other materials obtained (8,39%). MD material presented the highest percentage of mullite phase (22,45%) and hematite phase (14,49%).

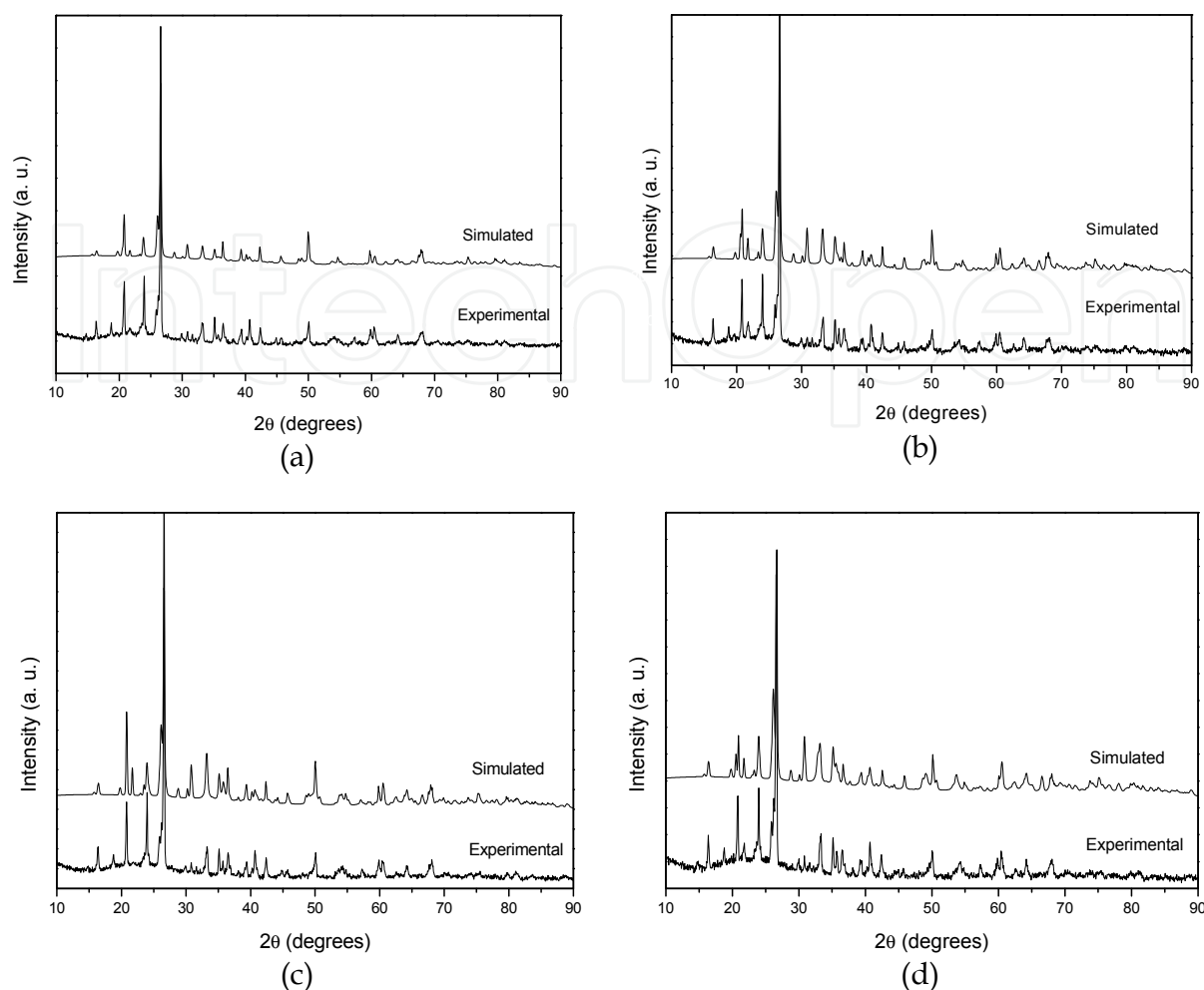


Fig. 6.4. Materials MA (a), MB (b), MC (c) and MD (d) patterns, experimental and simulated by the Rietveld Method.

Sample	$R_P^*$ (%)	$R_{W-P}^*$ (%)	$R_{EXP}^*$ (%)	Relative percentage of the crystalline phases calculated by Rietveld Method				
				$\alpha$ -Quartz	Silicon oxide	Tridimite	Mullite	Hematite
MA	7,41	9,97	3,32	54,89	21,32	3,31	15,91	4,58
MB	7,27	10,23	3,19	39,90	19,92	7,20	23,25	9,73
MC	8,92	12,39	3,22	37,76	18,66	8,39	19,95	15,24
MD	8,66	13,0	3,18	29,11	21,11	6,05	26,56	17,14

Table 6.6. Statistical numeric indicators  $R_P$ ,  $R_{WP}$  e  $R_{EXP}$  and related percentage calculated through Rietveld of crystalline phases.

The structural refinement of MA material presented the lowest of  $R_{W-P}$  (9,97%). Convergence was verified through indexes  $R_P$  e  $R_{WP}$ . In despite of the fact that  $R_P$  e  $R_{WP}$  are distant for more than the recommended 20%, experimental and simulated spectrum curves presented a good correspondence (Figure 6.4a), and the  $R_{WP}$  value is within the recommended range for good results ( $2 \leq R_{WP} \leq 10$ ).

Pattern of MB material presented a good approaching between the simulated diffraction pattern and the observed one, with a good definition to the intensities and peak positions, as shown in Figure 6.4b. Refinement quality indicators are  $R_P = 7,27\%$ ,  $R_{WP} = 10,23\%$  and  $R_{EXP} = 3,19\%$ .

It is possible to observe that, to MC material, there is also a larger difference between peaks intensities than in the pattern, experimental and simulated in the lower angles region, where more intense peaks are placed (Figure 6.4c). Refinement quality was evaluated through  $R_P$  e  $R_{WP}$  indexes, equals to  $8,92\%$  and  $12,39\%$ , respectively, while  $R_{EXP}$  was  $3,22\%$ . In despite of the difference between entre  $R_{W-P}$  and  $R_{EXP}$  is higher than the recommended  $20\%$ , simulated and experimental spectrum curves present good concordance, and the  $R_{W-P}$  value is within the recommended range in literature (Mccusker, & Von Drelle, 1990).

Crystalline phases structural refinement of MD material was the one that presented the highest  $R_{WP}$  value ( $13,0\%$ ) compared with the structural refinement done in the other materials. Convergence Indexes  $R_P$  e  $R_{EXP}$  were equal to  $8,66\%$ , and  $3,18\%$  respectively.

## 7. Conclusion

The methodology for quantification of the crystalline phases by Rietveld Methods was applied to ceramics materials and raw materials. The crystalline phases formation is related with the sintering process. The Rietveld method allows, simultaneously, perform unit cell refinement, refinement of crystal structure, microstructure analysis, quantitative analysis of phases and determination of preferred orientation. With the advancement of computer technology, the Rietveld method has allowed more information could be extracted from XRD patterns. Analyzing all the diffraction pattern and using the individual intensities of each angular step, the method enabled the refinement of complex crystal structures, and later applied to the provision of quantitative data accurately recognized.

Rietveld Method, due to the fact of using all X-ray diffraction profile in calculations, overcomes several compounds peaks superposition problem and turns possible to obtain results from all crystalline phases simultaneously, without the need of pattern samples and calibrations curves. It means an expressive gain in relation to other techniques to multiphase systems crystalline phases quantification through X-ray diffraction.

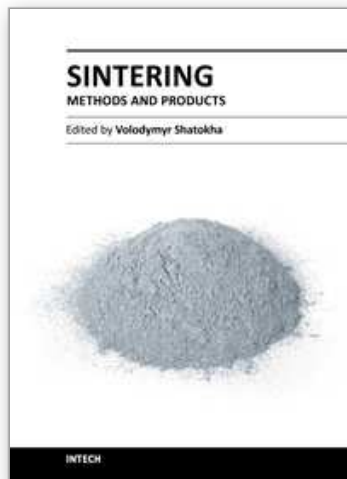
## 8. References

- Alégre, R. (1965). Généralisation de la méthode d'addition pour l'analyse quantitative par diffraction X. *Bull. Soc. Franc. Miner. Crist.* v. 88, p. 569-574.
- Borba, C. D. G. (2000). *Obtenção e caracterização de vitrocerâmicos de nefelina: medição de tamanho de cristalito e quantificação de fases por difração de raios-X*. Florianópolis, SC, Abr, 137p. Tese de Doutorado em Ciência e Engenharia de Materiais. Universidade Federal de Santa Catarina.
- Brindley, G. W., Brown, G. (1980). *Crystal structures of clay minerals and their X-ray identification*. London: Mineralogical Society, 495 p.
- Callister, W. D. (2002). *Materials Science and Engineering, an Introduction*. New York, John Wiley & Sons, Inc.

- Carvalho, F. M. S. (1996). *Refinamento da estrutura cristalina do quartzo, coríndon e criptomelana utilizando o método de Rietveld*. São Paulo, 73 p. Dissertação de mestrado. Instituto de Geociências da Universidade de São Paulo.
- Chung, F. H. (1974). Quantitative interpretation of X-ray diffraction patterns of mixtures. I. Matrix flushing method for quantitative multicomponent analysis. *Journal of Applied Crystallographic*. v.7, p.519-525.
- Coelho, C. (2002). *Quantificação de fases mineralógicas de matérias-primas cerâmicas via numérica*. Florianópolis, SC, Mai, 91p. Tese de Doutorado em Ciência e Engenharia de Materiais. Universidade Federal de Santa Catarina
- Cullity, B. C. (1978). *Elements of X-Ray diffracction*. New York: Addison-Wesley, Ed.2, 555p.
- Fabbri, B., Fiori, C., Ravaglioli, A. (1989). *Materie prime ceramiche: tecniche analitiche e indagini di laboratorio*. Faenza Editrice, v.3, 531p. 1989.
- Fleurence, A. (1968). *Analyse diffractométrique aux rayons X. Industrie Céramique*. n. 605, p. 203-211.
- Fonseca, A. T. (2000). *Técnicas de processamento cerâmico*. Lisboa: Universidade Aberta, 554p.
- Gobbo, L. A. (2003). *Os compostos do Clínquer Portland: sua Quantificação por Difração de Rios X e Quantificação por Refinamento de Rietveld*. Dissertação de Mestrado. Instituto de Recursos Minerais e Hidrogeologia. Universidade de São Paulo.
- Hald, P. (1952). *Técnica de la cerámica*. Barcelona: Ediciones. Omega, 126p.
- ICSD (Inorganic Crystal Structure Database) (1995). Gmchin-Intitut fur Anorganische Chemie and Fachinformationzentrum FIZ. Karlsruhe, Germany.
- International tables for x-ray crystallography (1997). International Union of Crystallography (IUCr).
- JCPDS (Joint Committee of Powder Diffraction Standards) (1981). International Centre for Diffraction Data. Pennsylvania, USA.
- Kingery, W. D., Bowen, H. K., Uhlmann, D. R. (1976). *Introduction to ceramics*. New York: John Wiley & Sons, Ed.2.
- Klug, H. P., Alexandder, L. E. (1954). *X-ray diffraction procedures for polycrystalline and amorphous materials*. Ed 2., 966p.
- Kniess, C.T. (2005). *Desenvolvimento e caracterização de materiais cerâmicos com adição de cinzas pesadas de carvão mineral*. 285p. Tese de Doutorado em Engenharia e Ciência dos Materiais. PGMat /Universidade Federal de Santa Catarina, Florianópolis.
- Kniess, C. T.; Prates, P. B.; Lima, J. C.; Kuhnen, N. C.; Riella, H. (2006). Influência da adição de cinzas pesadas de carvão na resistência mecânica à flexão de revestimentos cerâmicos. In: *50º Congresso Brasileiro de Cerâmica*, Blumenau. Anais do 50º Congresso Brasileiro de Cerâmica.
- Kniess, C. T.; Prates, P. B.; Lima, J. C.; Kuhnen, N. C.; Riella, H. (2007). Dilithium dialuminium trisilicate phase obtained using coal bottom ash. *Journal of Non-Crystalline Solids*, v. 353, p. 4819-4822.
- Kniess, C. T.; Prates, P. B.; Kuhnen, N. C.; Riella, H; Lima, J. C.; Franjdlich, E. U. (2009a). Determination of the Amorphous and Crystalline Phases of the Ceramic Materials. In: *11 th International Conference on Advanced Materials - ICAM 2009*, Rio de Janeiro, Brazil.
- Kniess, C. T.; Prates, P. B.; Milanez, K.; Kuhnen, N. C.; Riella; Lima, J. C.; Maliska, A. M. (2009b). Quantitative Determination of the Crystalline Phases of the Ceramic



- Materials Utilizing the Rietveld Method. In: *Seventh International Latin American Conference on Powder Technology (PTECH)*, Atibaia, Brazil.
- Kniess, C. T.; Riella, H; Franjdlich, E. U; Durazzo, M.; Saliba-Silva, A; Prestes, L. (2010). Determination of Crystalline Phases in the Uranium Silicide by X-ray Diffraction. In: *International Meeting on Reduced Enrichment for Research and Test Reactors - RERTR 2010; 32nd*, Lisboa, Portugal.
- L. D. Mccusker, R. B. Von Drelle, D. E. Cox, D. Louer, P. Scardi. (1990). *Journal of Applied Crystallographic*. v. 32, p. 36-50.
- Navarro, J. M. F. (1991). *El Vidrio*. Madrid: CSIC (Consejo Superior de Investigaciones Científicas).
- Padilha, A. F. (1997). *Materiais de Engenharia – Microestrutura e propriedades*. São Paulo: Hemus.
- Paiva-Santos, C.O. (1990). *Estudos de Cerâmicas Piezelétricas pelo método de Rietveld com dados de difração de raios X*. São Carlos, SP. Tese de doutorado. Instituto de Física e Química de São Carlos – Universidade de São Paulo.
- Paiva-Santos, C. O. (2001). *Caracterização de materiais pelo método de Rietveld com dados de difração por policristais*. São Paulo: Instituto de Química, UNESP, 46p.
- Paiva-Santos, C. O. (2005). *Aplicações do Método de Rietveld*. São Paulo: Instituto de Química, UNESP, 2005.
- Post, J. E., Bish, D. L. (1989). Rietveld refinement of crystal structures using power X-ray diffraction data. *Modern Power Diffraction. Mineralogical Society of America*. v.20. p. 277-308, 1989.
- Riello, P., Faguerazzi, G., Canton, P., Clemente, D., Signoretto, M. (1995). Determining the degree of crystallinity in semicrystalline materials by means of the Rietveld analysis. *Journal of Applied Crystallographic*. v. 28, p.121-126.
- Rietveld, H. M. (1967). Line profiles of neutron powder-diffraction peaks for structure refinement. *Acta Crystallographica* . n.22, p.151-1152, 1967.
- Rietveld, H. M. (1969). A profile refinement method for nuclear and magnetic structures. *Journal of Applied Crystallographic*, v.2, p.65-71, 1969.
- Warren, E. B. (1959). *X ray Diffraction*. London: Addison-Wesley Pub. Company.
- Wiles, D. B., Young, R. A. (1981). A new computer program for Rietveld analysis of X-ray powder diffraction pattern. *Journal of Applied Crystallographic*. v.14, p.149-151.
- Young, R. A. (1995). *The Rietveld Method*. New York: Oxford University Press, 298p.
- Young, R.A., Larson, A.C, Paiva-Santos, C.O. (1998). *Rietveld analysis of x-ray and neutron powder diffraction patterns*. Atlanta: School of Physics, Georgia Institute of Technology.



## **Sintering - Methods and Products**

Edited by Dr. Volodymyr Shatokha

ISBN 978-953-51-0371-4

Hard cover, 316 pages

**Publisher** InTech

**Published online** 23, March, 2012

**Published in print edition** March, 2012

This book is addressed to a large and multidisciplinary audience of researchers and students dealing with or interested in sintering. Though commonly known as a method for production of objects from fines or powders, sintering is a very complex physicochemical phenomenon. It is complex because it involves a number of phenomena exhibiting themselves in various heterogeneous material systems, in a wide temperature range, and in different physical states. It is multidisciplinary research area because understanding of sintering requires a broad knowledge - from solid state physics and fluid dynamics to thermodynamics and kinetics of chemical reactions. Finally, sintering is not only a phenomenon. As a material processing method, sintering embraces the wide group of technologies used to obtain such different products as for example iron ore agglomerate and luminescent powders. As a matter of fact, this publication is a rare opportunity to connect the researchers involved in different domains of sintering in a single book.

### **How to reference**

In order to correctly reference this scholarly work, feel free to copy and paste the following:

Cláudia T. Kniess, João Cardoso de Lima and Patrícia B. Prates (2012). The Quantification of Crystalline Phases in Materials: Applications of Rietveld Method, Sintering - Methods and Products, Dr. Volodymyr Shatokha (Ed.), ISBN: 978-953-51-0371-4, InTech, Available from:  
<http://www.intechopen.com/books/sintering-methods-and-products/the-quantification-of-crystalline-phases-in-materials-applications-of-rietveld-method>

**INTECH**  
open science | open minds

### **InTech Europe**

University Campus STeP Ri  
Slavka Krautzeka 83/A  
51000 Rijeka, Croatia  
Phone: +385 (51) 770 447  
Fax: +385 (51) 686 166  
[www.intechopen.com](http://www.intechopen.com)

### **InTech China**

Unit 405, Office Block, Hotel Equatorial Shanghai  
No.65, Yan An Road (West), Shanghai, 200040, China  
中国上海市延安西路65号上海国际贵都大饭店办公楼405单元  
Phone: +86-21-62489820  
Fax: +86-21-62489821

© 2012 The Author(s). Licensee IntechOpen. This is an open access article distributed under the terms of the [Creative Commons Attribution 3.0 License](#), which permits unrestricted use, distribution, and reproduction in any medium, provided the original work is properly cited.

IntechOpen

IntechOpen